

# Preparation and Solid State-Structure of the 1,3,5-Triazine-Bridged Tris(1,2,3,5-dithiadiazolyl) [ $N_3C_3(CN_2S_2)_3$ ]

A. W. Cordes,<sup>1a</sup> R. C. Haddon,<sup>1b</sup> R. G. Hicks,<sup>1c</sup> D. K. Kennepohl,<sup>1c</sup> R. T. Oakley,<sup>1,c</sup> L. F. Schneemeyer,<sup>1b</sup> and J. V. Waszczak<sup>1b</sup>

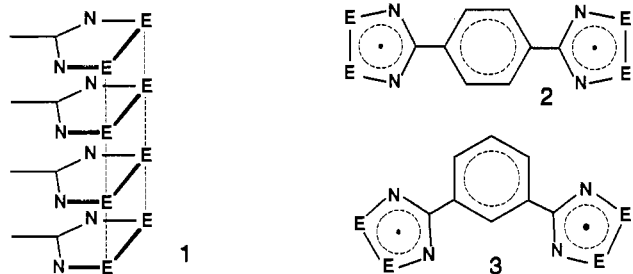
Department of Chemistry and Biochemistry, University of Arkansas, Fayetteville, Arkansas 72701, AT&T Bell Laboratories, Murray Hill, New Jersey 07974, and Guelph Waterloo Centre for Graduate Work in Chemistry, Guelph Campus, Department of Chemistry and Biochemistry, University of Guelph, Guelph, Ontario N1G 2W1, Canada

Received August 11, 1992

The preparation and solid-state characterization of the 1,3,5-triazine-bridged tris(1,2,3,5-dithiadiazolyl) complex 4,4',4''-(2,4,6-(1,3,5-triazinetriyl))tris(1,2,3,5-dithiadiazolyl) [ $N_3C_3(CN_2S_2)_3$ ] are described. The crystals belong to the monoclinic space group  $C2/c$ , with  $a = 20.759(7)$  Å,  $b = 10.525(3)$  Å,  $c = 17.554(3)$  Å,  $\beta = 140.18(4)^\circ$ ,  $fw = 390.5$ ,  $Z = 8$ , and  $V = 2456.2(12)$  Å<sup>3</sup>. The crystal structure consists of layers of interlocked dimers. Alternate layers are oriented in an antiparallel fashion, thereby precluding a stacked structure similar to that found in the related 1,3,5-benzene-based triradical. There are two dimerization environments. In one of these there are two equivalent interannular S - -S contacts of 3.069(4) Å, while in the other there are both long (3.225(4) Å) and short (2.872(4) Å) interannular S - -S contacts. The antiparallel layered structure leads to a skewed stacking arrangement in which the close interdimer S - -S contacts are 3.736(4) and 3.784(4) Å. In addition to the latter interactions, there are numerous lateral interdimer S - -S contacts close to or within the van der Waals range.

## Introduction

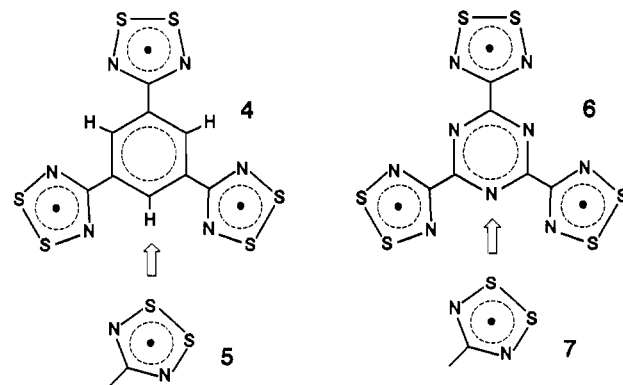
Interest in the design of molecular conductors based on neutral<sup>2</sup> rather than charged radicals has led us to explore the structural properties of polyfunctional 1,2,3,5-dithiadiazolyl and 1,2,3,5-diselenadiazolyl systems.<sup>3</sup> The architectural strategy we have followed involves the design of molecular "building blocks" which, in the solid state, adopt stacked structures (e.g., 1) with strong



intra- and interstack interactions. While tightly bound structures can be generated from bifunctional radicals based on the 1,4- and 1,3-phenylene-bridged systems, persuading molecular systems to adopt a stacked packing pattern is not an easy task.<sup>4</sup> The crystal structures of the 1,4-derivatives 2 (E = S, Se), for example, consist of dimers packed in a herringbone-like fashion.<sup>5</sup> Stacks of diradical units, linked vertically through alternate ends, are observed in the  $\alpha$ -phase of the 1,3-derivatives (E = S, Se),<sup>6</sup> but

in the  $\beta$ -phase of 3 (E = Se) the radicals associate as dimers which coil together to generate a chainlike motif.<sup>7</sup> Recently, we prepared the trifunctional radical 1,3,5-benzenetris(1,2,3,5-dithiadiazolyl) (4),<sup>8</sup> which does adopt a stacked radical packing arrangement similar to that found for 3 (E = S).

Although the structure of 4 exhibits many short intra- and interstack S - -S contacts, the density of the packing is limited by CH - -S interactions, which buffer the approach of neighboring rings (e.g., 5). In the belief that a tighter, smaller band gap structure might be obtained by the elimination of these buffering contacts, we have prepared and structurally characterized the related 1,3,5-triazine-2,4,6-tris(1,2,3,5-dithiadiazolyl) radical [4,4',4''-(2,4,6-(1,3,5-triazinetriyl))tris(1,2,3,5-dithiadiazolyl)] (6), in which the CH - -S interactions found in 4 are replaced by N - -S contacts (e.g., 7). Herein we describe the preparation and solid-state structural analysis of 6.



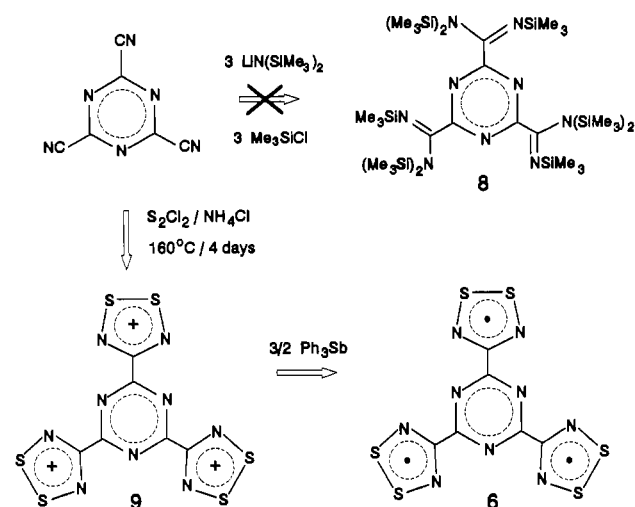
## Results

**Synthesis.** Our attempts to prepare 6 in a manner analogous to that used for other monofunctional and bifunctional dithia-

- (1) (a) University of Arkansas. (b) AT&T Bell Laboratories. (c) University of Guelph.  
 (2) (a) Haddon, R. C. *Aust. J. Chem.* **1975**, *28*, 2343. (b) Haddon, R. C. *Nature (London)* **1975**, *256*, 394.  
 (3) Cordes, A. W.; Haddon, R. C.; Oakley, R. T. In *The Chemistry of Inorganic Ring Systems*; Steudel, R., Ed.; Elsevier: Amsterdam, 1992; p 295.  
 (4) Enkelmann, V. *Angew. Chem., Int. Ed. Engl.* **1991**, *30*, 1121.  
 (5) Cordes, A. W.; Haddon, R. C.; Oakley, R. T.; Schneemeyer, L. F.; Waszczak, J. V.; Young, K. M.; Zimmerman, N. M. *J. Am. Chem. Soc.* **1991**, *113*, 582.  
 (6) Andrews, M. P.; Cordes, A. W.; Douglass, D. C.; Fleming, R. M.; Glarum, S. H.; Haddon, R. C.; Marsh, P.; Oakley, R. T.; Palstra, T. T. M.; Schneemeyer, L. F.; Trucks, G. W.; Tycko, R.; Waszczak, J. V.; Young, K. M.; Zimmerman, N. M. *J. Am. Chem. Soc.* **1991**, *113*, 3559.

- (7) Cordes, A. W.; Haddon, R. C.; Hicks, R. G.; Oakley, R. T.; Palstra, T. T. M.; Schneemeyer, L. F.; Waszczak, J. V. *J. Am. Chem. Soc.* **1992**, *114*, 1729.  
 (8) Cordes, A. W.; Haddon, R. C.; Hicks, R. G.; Oakley, R. T.; Palstra, T. T. M.; Schneemeyer, L. F.; Waszczak, J. V. *J. Am. Chem. Soc.* **1992**, *114*, 5000.

## Scheme I



diazolyl radicals<sup>5,6,9</sup> were thwarted by an inability to prepare the necessary starting material, *N,N,N',N'',N''',N''''*-nonakis(trimethylsilyl)-1,3,5-triazine-2,4,6-tricarboxamide (**8**). Treatment of 2,4,6-tricyanotriazine with 3 equiv of lithium bis(trimethylsilyl)amide inevitably led to attack of the amide at the endocyclic carbons rather than at the exocyclic nitriles.<sup>10</sup> Eventually, however, we developed an alternate route, albeit one which required more forcing conditions. By heating tricyanotriazine in refluxing sulfur monochloride for 4 days in the presence of excess ammonium chloride, we were able to effect addition of "[SSN]<sup>+</sup>" to the each of the three cyano groups. The product was the 1,3,5-triazine-2,4,6-triyltris(1,2,3,5-dithiadiazolium) tri-cation (**9**, as its chloride salt). This reaction, which represents a modification of the known method for effecting single addition to simple nitriles,<sup>11</sup> augers well for the preparation of other polyfunctional dithiadiazolium cations which are not readily accessible by the amidine methodology. Reduction of the trication with triphenylantimony yielded **6** as a black powder, which was purified by high-vacuum sublimation at 270 °C/10<sup>-2</sup> Torr to yield small metallic gray blocks.

**Crystal Structure of 6.** Crystals of **6** belong to the monoclinic space group *C2/c*. Atom coordinates are provided in Table I; internal bond lengths and angles are compiled in Table II. An ORTEP drawing of a single dimer unit, giving the atom-numbering scheme, is shown in Figure 1. Within the overall dimer unit, two [CN<sub>2</sub>S<sub>2</sub>]<sub>2</sub> "heads" are related by a 2-fold axis. Within these heads, the two interannular S...S contacts, S2...S5' (2.872(4) Å) and S1...S6' (3.225(4) Å) are markedly different. In the remaining head, the two interannular contacts (S3...S4' = 3.069(4) Å) are equal by symmetry.

The crystal symmetry affords a packing pattern in which the building blocks (the dimer units shown in Figure 1) are ordered in a head-to-tail fashion in rows which run along a 2-fold axis parallel to *y*. The motif produced is shown in Figure 2. The crucial difference between this structure and that of **4** is in the way in which consecutive layers are oriented; in an idealized stack, consecutive layers would fall directly above that shown in Figure 2. In the present case, however, consecutive layers run in an antiparallel fashion, producing the local arrangement illustrated in Figure 3. This packing produces a sandwich effect which traps the S3-S4/S4-S3 dimer head between two triazine rings (above and below). It also brings into stacking alignment, although in a less than ideal fashion, consecutive S1-S1/S6-S5

Table I. Atomic Parameters *x*, *y*, and *z* and *B*<sub>iso</sub><sup>a</sup>

	<i>x</i>	<i>y</i>	<i>z</i>	<i>B</i> <sub>iso</sub> , Å <sup>2</sup>
S1	-0.18134(14)	0.65700(15)	0.29457(15)	2.74(14)
S2	-0.17672(13)	0.83669(15)	0.35194(15)	2.41(13)
S3	-0.12863(14)	1.44646(17)	0.17344(18)	3.62(16)
S4	-0.09698(14)	1.44209(16)	0.08460(17)	3.42(17)
S5	-0.03705(13)	0.83544(15)	-0.06993(14)	2.38(12)
S6	-0.05839(13)	0.65551(14)	-0.04037(15)	2.51(15)
N1	-0.1657(4)	0.7135(5)	0.2230(5)	2.4(5)
N2	-0.1720(4)	0.9135(5)	0.2762(4)	2.2(4)
N3	-0.1371(4)	1.2920(5)	0.1733(5)	3.0(7)
N4	-0.1009(4)	1.2879(5)	0.0759(5)	2.8(5)
N5	-0.0645(4)	0.9082(4)	-0.0174(5)	2.1(4)
N6	-0.0841(4)	0.7103(5)	0.0223(5)	2.3(5)
N7	-0.1480(4)	1.0325(5)	0.1657(4)	2.0(4)
N8	-0.1036(4)	1.0304(5)	0.0758(4)	2.1(4)
N9	-0.1296(3)	0.8346(4)	0.1177(4)	1.9(4)
C1	-0.1635(4)	0.8404(5)	0.2231(5)	1.8(4)
C2	-0.1215(4)	1.2303(6)	0.1232(5)	2.2(6)
C3	-0.0830(4)	0.8361(5)	0.0257(5)	1.7(4)
C4	-0.1472(4)	0.9050(5)	0.1638(5)	1.8(5)
C5	-0.1243(4)	1.0893(5)	0.1216(5)	1.7(5)
C6	-0.1074(4)	0.9022(5)	0.0760(5)	1.6(4)

<sup>a</sup> Esd's refer to the last digit. *B*<sub>iso</sub> is the mean of the principal axes of the thermal ellipsoid.

Table II. Intramolecular Distances (Å) and Angles (deg)

Distances			
S1-S2	2.1099(24)	N4-C2	1.335(8)
S1-N1	1.633(5)	N5-C3	1.320(7)
S2-N2	1.621(5)	N6-C3	1.325(7)
S3-S4	2.107(3)	N7-C4	1.343(7)
S3-N3	1.635(6)	N7-C5	1.335(7)
S4-N4	1.626(5)	N8-C5	1.322(8)
S5-S6	2.0988(23)	N8-C6	1.351(7)
S5-N5	1.603(5)	N9-C4	1.338(7)
S6-N6	1.652(5)	N9-C6	1.332(7)
N1-C1	1.337(8)	C1-C4	1.484(8)
N2-C1	1.322(8)	C2-C5	1.485(8)
N3-C2	1.320(8)	C3-C6	1.484(8)
Angles			
S2-S1-N1	94.49(20)	N2-C1-C4	117.1(5)
S1-S2-N2	93.72(19)	N3-C2-N4	123.4(6)
S4-S3-N3	94.12(22)	N3-C2-C5	118.5(5)
S3-S4-N4	93.99(22)	N4-C2-C5	118.0(5)
S6-S5-N5	93.04(18)	N5-C3-N6	123.4(5)
S5-S6-N6	94.98(19)	N5-C3-C6	117.0(5)
S1-N1-C1	112.9(4)	N6-C3-C6	119.6(5)
S2-N2-C1	114.4(4)	N7-C4-N9	125.6(5)
S3-N3-C2	114.1(5)	N7-C4-C1	115.2(5)
S4-N4-C2	114.3(5)	N9-C4-C1	119.1(5)
S5-N5-C3	116.3(4)	N7-C5-N8	125.4(5)
S6-N6-C3	112.1(4)	N7-C5-C2	117.7(5)
C4-N7-C5	114.6(5)	N8-C5-C2	117.0(5)
C5-N8-C6	114.9(5)	N8-C6-N9	125.4(5)
C4-N9-C6	114.0(5)	N8-C6-C3	114.8(5)
N1-C1-N2	124.1(5)	N9-C6-C3	119.8(5)
N1-C1-C4	118.8(5)		

dimers. The stacking pattern produced, when viewed from a direction parallel to *z*, is shown in Figure 4.

The packing of dimers summarized above gives rise to a large number of close (i.e., near or within the van der Waals range)<sup>12</sup> interdimer S...S contacts, all of which are defined in Table III. Of particular note are the head-to-tail contacts *d*<sub>1</sub> (3.769(3) Å) and *d*<sub>2</sub> (3.633(3) Å), the latter being the shortest such contact in the structure. In addition to the close contacts between the S3/S4 heads and the pocket of the adjacent dimer, the S3/S4 units are also involved in a number of close lateral S...S interactions (*d*<sub>10</sub>-*d*<sub>12</sub>) with the dimers in adjacent rows (see Figure 5).

**Magnetic Measurements and Conductivity.** The measured magnetic susceptibility of **6** as a function of temperature is shown

(9) Del Bel Belluz, P.; Cordes, A. W.; Kristof, E. M.; Kristof, P. V.; Liblong, S. W.; Oakley, R. T. *J. Am. Chem. Soc.* **1989**, *111*, 9276.

(10) We have found that tricyanotriazine also reacts rapidly with ammonia to afford cyanodiaminotriazine.

(11) Alange, G. G.; Banister, A. J.; Bell, B.; Millen, P. W. *J. Chem. Soc., Perkin Trans. 1* **1979**, 1192.

(12) Bondi, A. *J. Phys. Chem.* **1964**, *68*, 441.

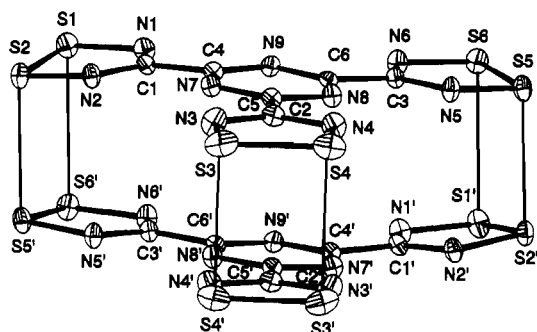


Figure 1. ORTEP drawing of a single triradical dimer of 6, with atom-numbering scheme.

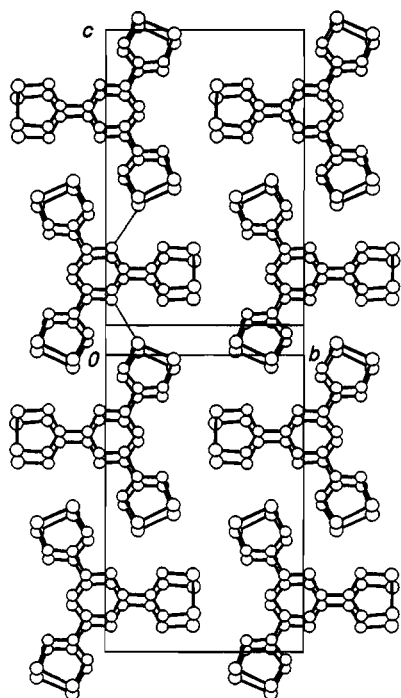


Figure 2. Packing of triradical dimers of 6 in the  $yz$  plane. The dashed lines indicate buffering N...S interactions.

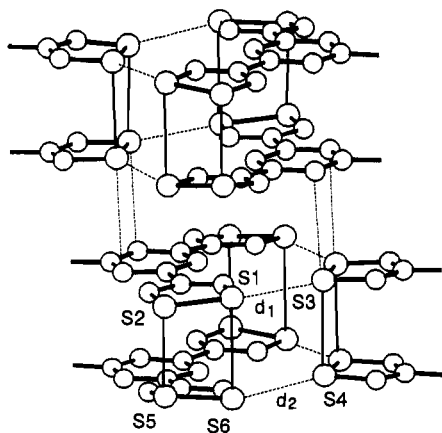


Figure 3. Head-over-tail packing of consecutive layers of triradicals in 6, showing lateral S...S contacts.

in Figure 6. As observed for 4, and also 2 and 3 ( $E = S$ ), the compound exhibits Curie behavior at low temperatures, consistent with the presence of low-level paramagnetic impurities. On the basis of a Curie-Weiss treatment of the magnetic data, the unpaired spin concentration amounts to 0.31% on a per molecule basis; the  $\Theta$  value is 1 K.

At elevated temperatures, the behavior of 6 resembles that found for 2 ( $E = S$ ); the magnetic susceptibility rises slowly but

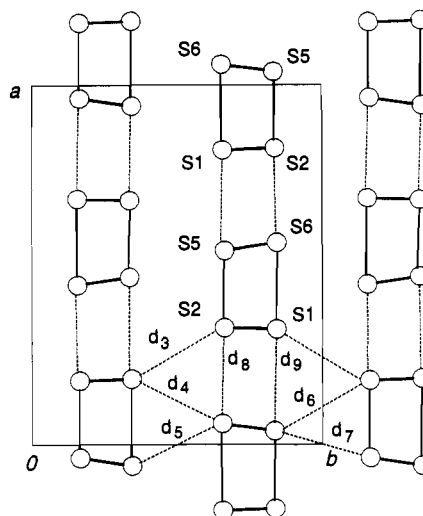


Figure 4. Lateral S...S contacts between pseudocolumns of radicals of 6.

Table III. Intradimer and Interdimer S...S Contacts (Å)

Intradimer					
As in Figure 1					
S1...S6'	3.225(4)	S2...S5'	2.872(4)	S3...S4'	3.069(4)
Interdimer					
As in Figure 3					
$d_1$	S1...S3''	3.769(3)	$d_2$	S6...S4''	3.633(3)
As in Figure 4					
$d_3$	S1...S2''	3.876(3)	$d_4$	S1...S6''	3.791(3)
$d_5$	S6...S6''	3.650(3)	$d_6$	S2...S5''	4.011(3)
$d_7$	S5...S5''	3.820(3)	$d_8$	S2...S6''	3.736(4)
$d_9$	S1...S5''	3.784(4)			
As in Figure 5					
$d_{10}$	S6...S3''	4.155(3)	$d_{11}$	S6...S4''	3.989(3)
$d_{12}$	S1...S4''	4.047(3)			

steadily above 450 K, with no indication of the large hysteretic increase in magnetization noted in 3 and, to a lesser extent, in 4. The sharp rise to a maximum near 640 K is associated with sample decomposition. Insofar as large paramagnetic enhancements are restricted to 3 and 4, we conclude that such behavior is structure related; the structures of 2 and 6 consist of discrete molecular dimers, as opposed to the zigzag polymeric networks observed in 3 and 4.

The small size and low conductivity of crystals of 6 precluded any accurate measurement of conductivity; preliminary measurements suggest  $10^{-8}$  S  $\text{cm}^{-1}$  as an upper bound.

## Discussion

The crystal structure of 4 consists of stacks of triradicals running parallel to the  $x$  axis. The unit cell (Figure 7) contains four such stacks, packed together in a pseudopinwheel fashion similar to that observed in the  $\alpha$ -phase of 3. The lattice symmetry distinguishes between the three radical rings in each triradical unit, thus affording the three columns labeled A-C. In modifying the molecular structure of 4 to 6, our intent was to retain the same solid-state packing pattern while at the same time enhancing the observed intercolumnar interactions by eliminating the buffering effect of CH...S repulsions.<sup>13</sup> Of the three symmetry-distinct radical rings, only B and C exhibit these close CH...S approaches (Table IV); ring A is well removed from the benzene

(13) It is worth noting that 1,3,5-triphenylbenzene and *s*-triphenyltriazine are not isomorphous either. In these two structures, however, there are quite significant differences in the molecular structures, notably the degrees of internal rotation (torsion) about the phenyl-benzene and phenyl-triazine C-C bonds: (a) Lin, Y. C.; Williams, D. E. *Acta Crystallogr.* **1975**, *B31*, 318. (b) Diamani, A.; Giglio, E.; Ripamonti, A. *Acta Crystallogr.* **1965**, *19*, 161.

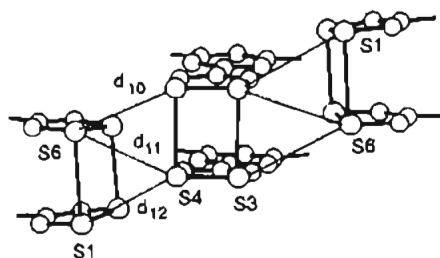


Figure 5. Lateral S-S contacts between radicals in 6.

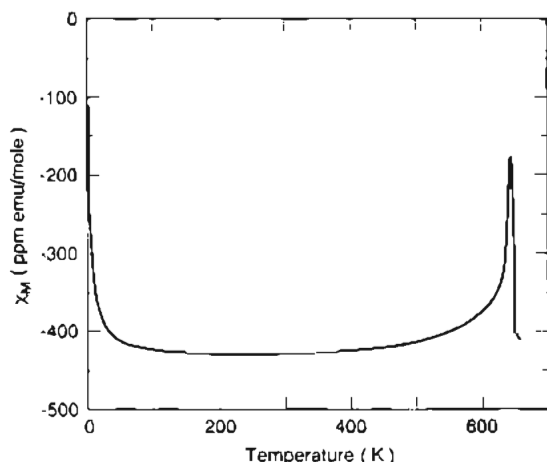
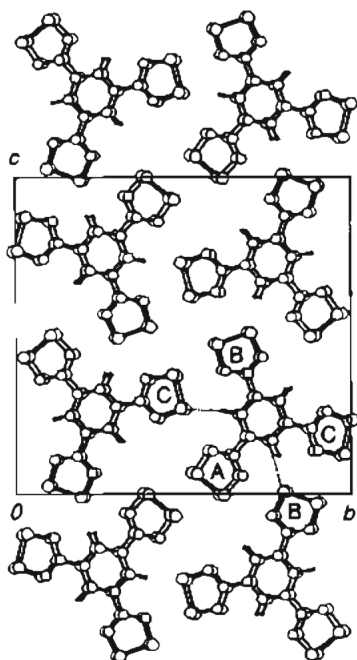


Figure 6. Magnetic susceptibility of 6 as a function of temperature.

Figure 7. Packing of 4, viewed parallel to the *x* axis. The dashed lines indicate buffering CH-S interactions.

periphery. Indeed, there is a notable void to either side of the A ring. If the triazine-based system 6 were to adopt the benzene-based structure 4, this void would become even more pronounced.

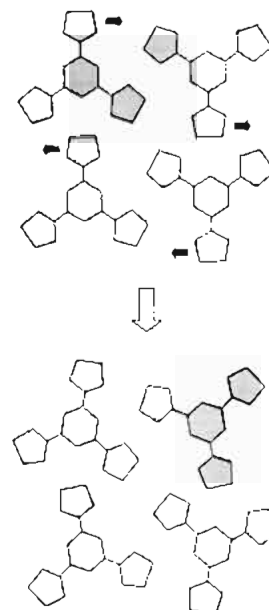
While we have not achieved our original structural objective, the reasons for the structural differences between 4 and 6 are readily apparent and serve as lessons for the future. As desired, the structure of 6 has a higher density ( $d_{\text{calcd}} = 2.11 \text{ g cm}^{-3}$ ) than that of 4 ( $d_{\text{calcd}} = 1.964 \text{ g cm}^{-3}$ ). Ironically, the increase is larger than expected and reflects a more efficient packing pattern, which is possibly only for 6. This higher density for 6 can be attributed in large measure to "in-plane" effects; i.e., the motif of Figure 2 is more closely knit than that shown in Figure 7. The origin of this denser packing can be seen upon comparison

Table IV. Buffering CH-S and N-S Contacts<sup>a</sup> (Å) in 4 and 6

Compound 4			
H8 <sup>b</sup> -S	-none	H14 <sup>b</sup> -S	-none
H10-S	2.858	H10-S	3.154
H12-S	3.045	H12-S	2.871
H16-S	2.946	H16-S	3.051
H18-S	2.733	H18-S	2.765
Compound 6			
N7-S	3.515	N9-S	-none
N8-S	3.247	N8-S	3.316

<sup>a</sup> Less than 3.5 Å for CH-S and 4.0 Å for N-S. <sup>b</sup> This atom lies in the void to either side of the A stacks (see Figure 7). <sup>c</sup> This atom lies in the void created by the head-to-tail packing (see Figure 2).

## Scheme II



of the lateral S-N and CH-S buffering contacts summarized in Table IV; the approach of heavy atoms (N and S) in 6 is much closer than is found (for C and S) in 4.<sup>14</sup> In addition, and in spite of the more densely packed motif found for 6, the N-S buffer distances are still well outside the van der Waals range; i.e., the arrangement of the building blocks suffers no lateral impediment. Replacement of N by CH with retention of this structure would, however, lead to severe CH-S repulsions between the rings. One way of alleviating such repulsions would be to induce sequential clockwise and anticlockwise rotation of consecutive blocks, as illustrated in Scheme II; this process unlocks the tight buffering interactions of the high-symmetry structure and generates the in-plane motif found in 4.

## Summary and Conclusion

Chemical modification of 4 to produce 6 induces a more dramatic solid-state effect than we had anticipated. The removal of the CH-S buffers in 4 allows a more efficient but more symmetrical packing motif for the molecular building blocks. The clustering of radicals in a pinwheel-like arrangement and the zigzag propagation of the bond-alternation waves in the resulting columnar stacks appear, at least in part, to result from, rather than in spite of, CH-S interactions. In the absence of these effects (as observed here), a higher symmetry packing motif, one not associated with columnar stacking, can be produced.

## Experimental Section

**Starting Materials and General Procedures.** Ethyl cyanofornate, dimethyl sulfoxide (DMSO), sulfur monochloride, and triphenylantimony were all obtained commercially (Aldrich). All solvents and sulfur

(14) When taken together with the C-H distances, the buffering effect of the CH-S contacts swells the C-S distances in 4 far beyond the N-S contacts found in 6.

monochloride were distilled before use. 2,4,6-Tricyano-1,3,5-triazine was prepared by literature methods<sup>15,16</sup> and was sublimed in vacuo prior to use. All reactions were performed under an atmosphere of nitrogen. Mass spectra were recorded on a Kratos MS890 mass spectrometer. Infrared spectra (CsI optics, Nujol mulls) were obtained on a Nicolet 20SX/C FTIR instrument. Elemental analyses were performed by MHW Laboratories, Phoenix, AZ.

**Preparation of 1,3,5-Triazine-2,4,6-triyltris(1,2,3,5-dithiadiazolyl) (6).**

A mixture of tricyanotriazine (1.02 g, 6.5 mmol) and finely powdered NH<sub>4</sub>Cl (4.0 g, 75 mmol) was refluxed in 40 mL of S<sub>2</sub>Cl<sub>2</sub> for 4 days. After the mixture was cooled to room temperature, the crude tris(dithiadiazolium) salt **9** was filtered off and washed with CH<sub>2</sub>Cl<sub>2</sub>. The crude solid was then slurried in 50 mL of CH<sub>2</sub>Cl<sub>2</sub>, and chlorine gas was bubbled through the mixture for 10 min. The orange solid was removed by filtration. This purging process, which had the effect of oxidizing all binary S<sub>2</sub>N<sub>2</sub> materials to S<sub>3</sub>N<sub>3</sub>Cl<sub>3</sub> (CH<sub>2</sub>Cl<sub>2</sub> soluble), was repeated a total of three times. The orange product, crude **8**, was then dried in vacuo (dec >230 °C). This chloride salt was reduced by treatment with excess Ph<sub>3</sub>Sb (4.5 g, 13 mmol) in refluxing CH<sub>3</sub>CN for 24 h. The black precipitate of crude **6** was filtered off, dried in vacuo, and purified by sublimation at 270 °C/10<sup>-5</sup> Torr as small metallic gray cubes (0.31 g, yield 12%), dec >350 °C. Larger crystals suitable for X-ray work were obtained by sealed-tube sublimation at 290 °C. Anal. Calcd for C<sub>6</sub>N<sub>9</sub>S<sub>6</sub>: C, 18.46; N, 32.28; S, 49.26. Found: C, 18.66; N, 32.17; S, 49.16. Mass spectrum (EI, *m/e*): 390 (M<sup>+</sup>, 38%), 344 ([M - SN]<sup>+</sup>, 13%), 312 ([M - S<sub>2</sub>N]<sup>+</sup>, 54%), 266 ([M - S<sub>3</sub>N<sub>2</sub>]<sup>+</sup>, 33%), 234 ([M - 2(S<sub>2</sub>N)]<sup>+</sup>), 38%), 156 ([M - 3(S<sub>2</sub>N)]<sup>+</sup>, 4%), 130 (CNCN<sub>2</sub>S<sub>2</sub><sup>+</sup>, 6%), 104 (CN<sub>2</sub>S<sub>2</sub><sup>+</sup>, 22%), 78 (S<sub>2</sub>N<sup>+</sup>, 55%), 64 (S<sub>2</sub><sup>+</sup>, 100%). IR (1600–250 cm<sup>-1</sup>): 1515 (vs), 1412 (w), 1340 (m), 1306 (s), 1261 (m), 1218 (w), 1009 (w), 831 (m), 795 (m), 771 (s), 762 (m), 742 (vs), 624 (w), 501 (vs) cm<sup>-1</sup>.

**X-ray Measurements.** All X-ray data were collected on an ENRAF-

**Table V.** Crystal Data for **6**

formula	S <sub>6</sub> N <sub>9</sub> C <sub>6</sub>	<i>d</i> (calcd), g cm <sup>-3</sup>	2.11
fw	390.5	space group	C2/c
<i>a</i> , Å	20.759(7)	<i>Z</i>	8
<i>b</i> , Å	10.525(3)	<i>λ</i> , Å	0.710 73
<i>c</i> , Å	17.554(3)	temp, K	293
<i>β</i> , deg	140.18(4)	<i>μ</i> , cm <sup>-1</sup>	10.8
<i>V</i> , Å <sup>3</sup>	2456.2(12)	<i>R</i> , <i>R</i> <sub>w</sub> <sup>a</sup>	0.068, 0.107

$$^a R = [\sum ||F_o| - |F_c||] / [\sum |F_o|]; R_w = \{[\sum w||F_o| - |F_c||^2] / [\sum (w|F_o|^2)]\}^{1/2}.$$

Nonius CAD-4 diffractometer at 293 K with monochromated Mo K $\alpha$  ( $\lambda = 0.710 73$  Å) radiation. Crystals were mounted on glass fibers with epoxy. The cell dimensions were obtained from seven reflections measured with  $2\theta$  in the range 52–56°. Data were collected with a  $\theta$ - $2\theta$  technique, and the structure was solved using direct methods and refined by full-matrix least-squares procedures which minimized  $\sum w(\Delta F)^2$ ; a summary of the crystal and structure solution data is provided in Table V. Full data collection and structure solution and refinement parameters are available as supplementary material.

**Magnetic Measurements.** The magnetic susceptibility of **6** was measured from 4.2 to about 650 K by using the Faraday technique. Details of the apparatus have been previously described.<sup>17</sup>

**Acknowledgment.** Financial support at Guelph was provided by the Natural Sciences and Engineering Research Council of Canada and at Arkansas by the National Science Foundation (EPSCOR Program).

**Supplementary Material Available:** Table S1, giving crystal data and structure solution and refinement parameters for **6**, and Table S2, listing anisotropic thermal parameters for **6** (3 pages). Ordering information is given on any current masthead page.

(15) Ott, E. *Ber. Dtsch. Chem. Ges.* **1919**, 656.

(16) Sugiyama, Y.; Sasaki, T.; Nagato, N. *J. Org. Chem.* **1978**, *43*, 4485.

(17) (a) DiSalvo, F. J.; Waszczak, J. V. *Phys. Rev.* **1981**, *B23*, 457. (b) DiSalvo, F. J.; Waszczak, J. V.; Tauc, J. *Phys. Rev.* **1972**, *B6*, 4574.